Integrating hybrid reinforced concrete technology and advanced FEM-based numerical modelling for crack control in long concrete foundations without joints.

Joaquim A. O. Barros[1], Tiago D. S. Valente[2], Inês G. Costa[2] and Felipe J. S. A. Melo[2]

[1] ISISE, Department of Civil Engineering, University of Minho, Azurém 4800-058 Guimarães, Portugal
[2] CiviTest – Pesquisa de Novos Materiais para a Engenharia Civil, Lda., 4770-160 Vila Nova de Famalicão, Portugal
barros@civil.uminho.pt

Abstract. The present work describes the analysis of a long and jointless concrete foundation reinforced with conventional steel meshes and discrete polypropylene fibers. A thermo-mechanical nonlinear transient simulation is performed to assess the cracking risk and magnitude of the fiber reinforced concrete (FRC) due to the heat development generated from the cement hydration in the early stages of the concrete hardening phase. The thermal and cracking material data considered in the constitutive model are calibrated from the experimental program conducted when casting the concrete foundation. The concrete shrinkage, viscoelasticity and maturity concepts are also considered in the analysis.

The results of the numerical simulations revealed an adequate performance of the hybrid reinforcement to limit the crack opening of the concrete foundation since early ages, while significantly reducing the conventional steel reinforcement ratio.

Keywords: Hybrid reinforcement, Polypropylene fibers, Finite Element Method, Thermo-mechanical analysis, Early ages.

1   Introduction

The use of hybrid reinforcements in concrete elements, combining discrete fibers and conventional steel bars, is seen as a promising solution to maximize the potentialities of both types of reinforcements. The use of this hybrid reinforcement was reported in foundations, beams, slabs, shells, among other structures [1]–[3].

It is well known that the addition of short and randomly distributed fibers in concrete increases its post-cracking resistance, ductility and energy absorption [4], [5]. Furthermore, the restrain to crack opening, provided by the different fiber reinforcement mechanisms at fracture, enhances the durability and integrity of concrete members. Based on these benefits, fiber reinforcements demonstrate a great potential to replace conventional steel reinforcements, particularly in structural members of high support redundancy.

The present work focusses in the study of a long and jointless concrete foundation member of an industrial equipment, submitted to relatively low level of external actions.

The geometry of the foundation is presented in Figure 1. The cross-section has a hollow concrete shape, with concrete walls with 200 mm of thickness. The total length of the foundation is 22.4 m. Reinforced concrete diaphragms of 100mm thickness are disposed at the extremities, ¼ and ½ of the foundation length for increasing transversal and torsional stiffness. The hollow core is formed by expanded polystyrene blocks (EPS), with 10 kg/m^3 of density. In order to the reduce the frictional restriction between the foundation and surrounding soil, a double layer of polyethylene sheets lubricated with mineral oil was placed in the bottom and lateral faces of the foundation.

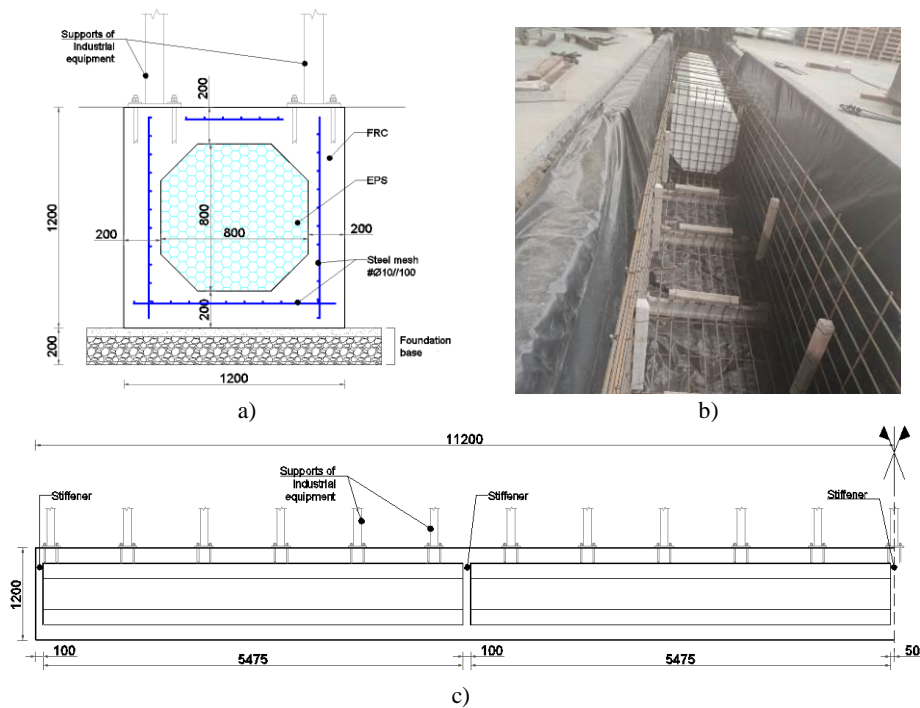a)   b)

c)

Figure 1 – Geometry of the foundation: a) Cross-section view; b) View of the positioning of the conventional reinforcements and EPS core; c) Longitudinal view of half of the foundation (dimensions in mm).

A hybrid reinforcement for the concrete parts of the foundation was defined at the design stage, formed by conventional steel meshes and discrete polypropylene fibers. The use of fibers aims to reduce the conventional reinforcement ratio, increasing the concrete post-cracking resistance and restraining crack opening, while increasing the durability of the foundation member by only one layer of conventional reinforcement with relatively high concrete cover thickness.

The concrete strength class C30/37 was chosen for the execution of the foundation, while at the design stage the toughness class 3c (classification of the a post-cracking behavior of a fiber reinforced concrete according to *fib* Model Code 2010 [6]) was prescribed, corresponding to a characteristic residual flexural strength for a crack mouth opening displacement (CMOD) equal to 0.5 mm of f_{R1k} =3 MPa and to CMOD=2.5 mm a value of f_{R3k} =2.7 MPa.

The adopted polypropylene fibers were fabricated by Exporplás – Indústria de Exportação de Plásticos, S.A, referenced as 1EST54, with an equivalent diameter of 0.7 mm, length equal to 54 mm, modulus of elasticity of 6 GPa and ultimate tensile strength of 500 MPa. In order to achieve the toughness class 3c, 6 kg/m³ of this type of fibers were used for producing the fiber reinforced concrete (FRC).

The adopted conventional reinforcement was formed by Ø10/100 mm squared steel mesh of the strength class A500NR. A minimum cover of 50 mm was adopted in order to minimize the susceptibility of steel bars to corrosion.

Due to the geometry of the structural member, particularly its length, the main cracking risk arises from the tensile strain gradient caused by the heat development generated by the cement hydration in the early stages of the concrete hardening phase and subsequent heat dissipation. The present work provides an integrated analysis, based on experimental and numerical studies, to assess the cracking risk of the foundation during the early ages of the concrete hardening phase.

2   Experimental study

The construction of the hybrid reinforced concrete (HRC) member included the material characterization of the evolution of the FRC mechanical properties since its early ages. In addition, a monitoring program was conducted to register the evolution of the temperature in some positions of the HRC foundation, during the early stages of the concrete hardening phase.

2.1   Material characterization

During the execution of the foundation, FRC samples were collected to determine the evolution with time of the compressive strength and post-cracking residual flexural strength.

The compressive strength of the FRC was evaluated on cubic samples of 100 mm edge, according to the standard NP EN 12390-3 [7], at the ages of 1, 4, 21 and 28 days after casting. The post-cracking residual flexural strength was determined from notched prismatic samples, submitted to 3-point bending, according to the standard EN 14651 [8], at the ages of 1, 4 and 21 days after casting.

The evolution of the average values of compressive strength is presented in Figure 2. The evolution of the compressive strength according to the maturity model presented in Eurocode 2 – Part 1-1 (EC2-1-1) [9] is also presented, which is determined from the following equation:

4

$$\begin{cases} f_{cm}(t) = \beta_{cc}(t) f_{cm} \\ \beta_{cc}(t) = \exp\left[s\left[1 - \left(\dfrac{28}{t}\right)^{0.5} \right] \right] \end{cases} \tag{1}$$

where t is time in days, and s is a coefficient that depends on the type of cement (for CEM II 42.5R, s=0.2).
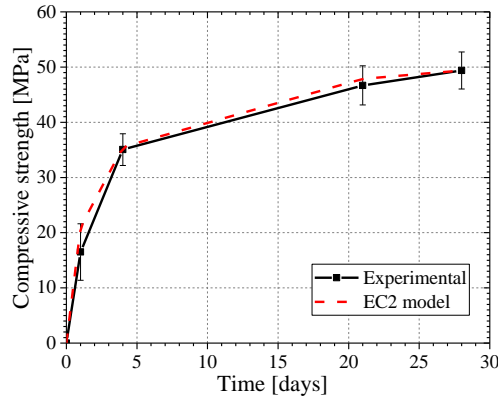

Figure 2 – Evolution of the average compressive strength, including standard deviation of tested samples for each age after casting.

Considering that the ratio between the compressive strength on cubic and cylindric samples is equal to $f_{cm,cubic}/f_{cm,cyl} = 0.8$ and that the characteristic compressive strength is equal to $f_{ck} = f_{cm} - 8MPa$, it is possible to verify that the developed FRC has characteristic compressive strength of 31.5 MPa, therefore it is of strength class C30/37.

The evolution of the average post-cracking residual flexural strength is presented in Figure 3, namely the average value of the residual flexural strength corresponding to a CMOD equal to 0.5 mm (f_{R1m}), 1.5 mm (f_{R2m}), 2.5 mm (f_{R3m}) and 3.5 mm (f_{R4m}).

The flexural residual strength of the FRC was also estimated for t=28 days, assuming an analogous evolution of FRC flexural residual strength as the one presented by Eq. (1) for the concrete compressive strength. The estimated results for t=28 days are also displayed in Figure 3.

Considering the ratio between the characteristic and average residual flexural strength equal to $f_{Rik}/f_{Rim} = 0.7$, as proposed in fib Model Code 2010 [6], it is possible to estimate that $f_{R1k} = 2.00MPa$ and $f_{R3k} = 2.71MPa$, which revels that the adopted FRC is of toughness class 2e, instead of the 3c, as prescribed in the design stage.
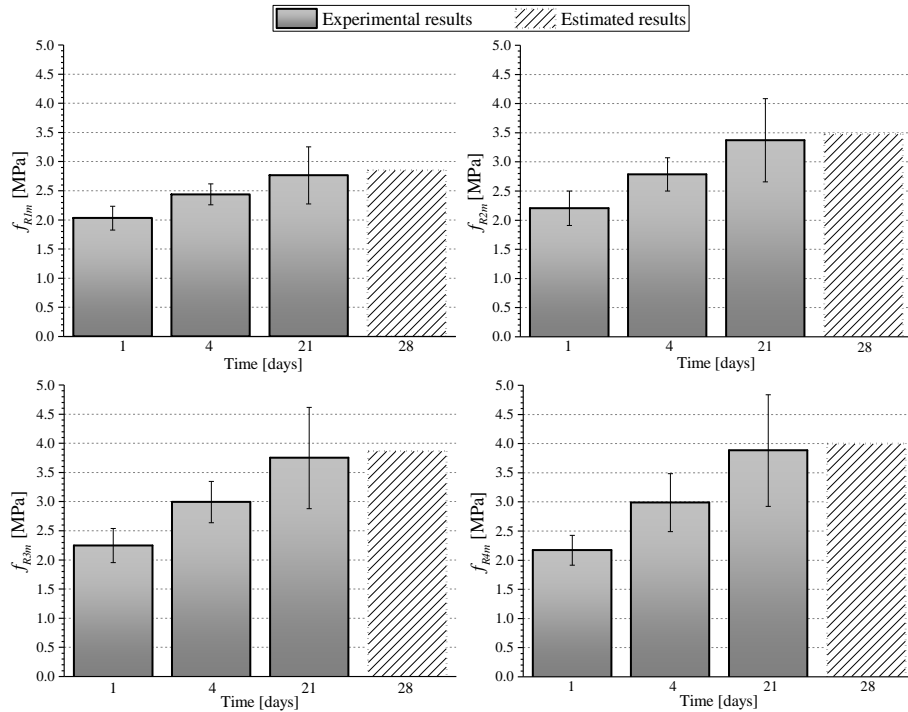
Figure 3 – Evolution of average values of the FRC residual flexural strength, including the standard deviation for each age after casting.

2.2 Measurement of temperature evolution in the HRC foundation

Previously to the FRC casting, thermocouple sensors were applied to capture the temperature evolution inside the HRC foundation, particularly during its initial hardening phase. The thermocouples were placed at 1.5 m from the middle cross-section of the foundation. The position and reference of the thermocouples in the cross-section is presented in Figure 4a**Error! Reference source not found.**.

Figure 4b presents the evolution of the temperature captured by the thermocouples placed inside the HRC foundation (TC_1 to TC_5) and also the external environment temperature captured by a thermocouple placed in the vicinity of the structural member (TC_6). The temperature was recorded up to 105 h (approximately 4 days) after FRC casting. The peak of temperature registered by the thermocouples was recorded at about 25 h after casting, with a maximum value of 44.1ºC (TC_1). In this period, the environment temperature ranged between 13.4ºC and 19.9ºC.
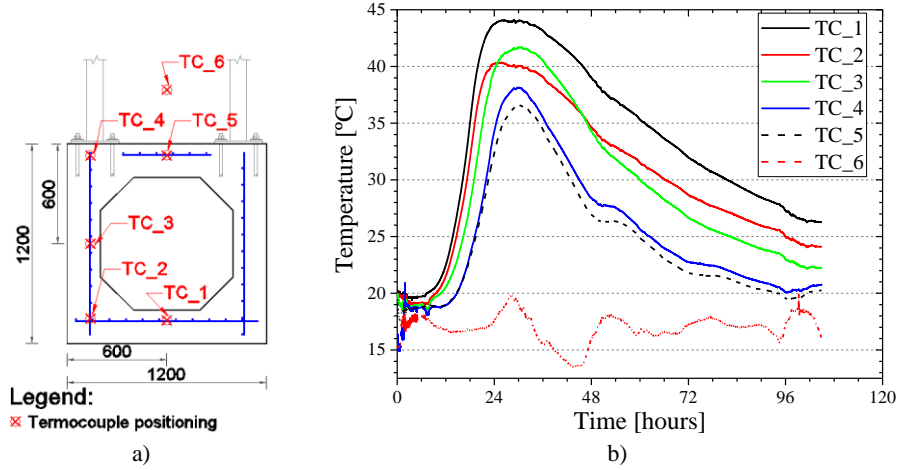
Figure 4 – a) Position and reference of the thermocouples in the cross-section at 1.5 m from the middle of the foundation (dimensions in mm); b) Evolution with time of the temperature inside the prototype and of the environment.

3   Numerical study

An integrated numerical study was developed for obtaining reliable information to capture the behavior of the HCR element presented in Figure 1, particularly to assess the cracking risk of FRC element due to the early age heat development.

In this scope, the numerical model parameters that describe the heat development due to the cement hydration of the FRC composition were calibrated based on the data collected from the experimental program.

Based on the results of the 3-point bending tests of the FRC, the stress crack width constitutive law of this FRC was derived by performing an inverse analysis.

The numerical simulation of the HRC foundation is presented considering the numerical models that describe the fracture behavior and heat development due to cement hydration, in order to investigate the behavior of the concrete element under analysis.

3.1   Calibration of thermal model parameters

The numerical model that describes the heat development of concrete due to cement hydration is described in [10], which is based on the mathematical formulation proposed by Reinhardt et al. [11] and on the Arrhenius law.

The unknown main model parameters correspond to the total accumulated heat of the cement hydration, Q_{total}, and to the normalized heat generation rate, $f(\alpha_T)$, that is a function of the degree of heat development. The cement content (kg/m^3), the apparent activation energy, E_a, that is dependent on the cement type, and the Arrhenius rate constant, A_T, are known model parameters: i) the FRC composition adopted 350 kg/m^3

of cement type CEM II/A-L 42.5R; ii) based on the data collected from [12], for this type of cement it can be assumed that $A_T = 52.05 \times 10^6$ and $E_a = 40.31 kJ/mol$.

In order to derive the unknown model parameters (Q_{total} and $f(\alpha_T)$), a numerical model of the foundation was developed for obtaining the temperature field in the structure and compare the numerical results with the experimental data recorded in the thermocouples installed in the element (section 2.2). A series of nonlinear thermal transient analysis were conducted with different sets of the model parameters to simulate the heat development of the initial 105 h of the cement hydration phase.

The numerical simulations were carried out in the Finite Element Model (FEM) software, FEMIX [13]. Only ¼ of the model was simulated, taking advantage from the double symmetry of the HRC foundation and surrounding soil. The model was formed with by solid finite elements of 20 nodes, namely 6376 to simulate the HRC foundation, 1024 to simulate the EPS core of the foundation, and 3168 to simulate the surrounding soil. It was adopted a Gauss Legendre integration scheme, with 2×2×2 integration points (IP's). The finite element mesh is presented in Figure 5.

The following values for the FRC properties in the thermal analysis were considered: thermal conductivity equal to 2.6 W/m.K; volumetric heat capacity equal to 2400 kJ/m³K. For the environmental temperature it was assumed the hourly average value of the environment temperature registered during the experimental tests.

The value of the heat transfer coefficient assigned to the face in contact with the environment is 10 W/m²K, while for the faces in contact with the plywood formwork (lateral faces of the concrete element) was adopted an heat transfer coefficient equal to 5.0 W/m²K (considering that the plywood thickness is equal to 20 mm and its thermal conductivity is equal to 0.2 W/m.K).

During the transient thermal analysis, it was considered that the concrete element is demolded at 48 hours after casting. Afterwards, it was assumed that all faces are exposed to environment and have a heat transfer coefficient equal to 10 W/m²K. During the entire duration of the analysis it is considered a 200 mm gap between the lateral faces of the foundation and the surrounding soil.

For the faces of the elements in the planes of symmetry and on the extremities boundaries of the model it was assumed an adiabatic boundary (heat transfer coefficient equal to 0.0 W/m²K).

The evolution of the temperature in the nodes of the mesh correspondents to the localization of the thermocouples was compared with the results collected during the experimental tests. As presented in Figure 6a, a good agreement between the numerical and the experimental results was obtained for $Q_{total} = 400 kJ/kg$ and for the normalized heat generation rate presented in Figure 6b.

In Figure 7 is presented the temperature field in the HRC foundation at t=25 h after casting, which corresponds to the instant that the maximum temperature was registered by the thermocouples in the experimental tests.
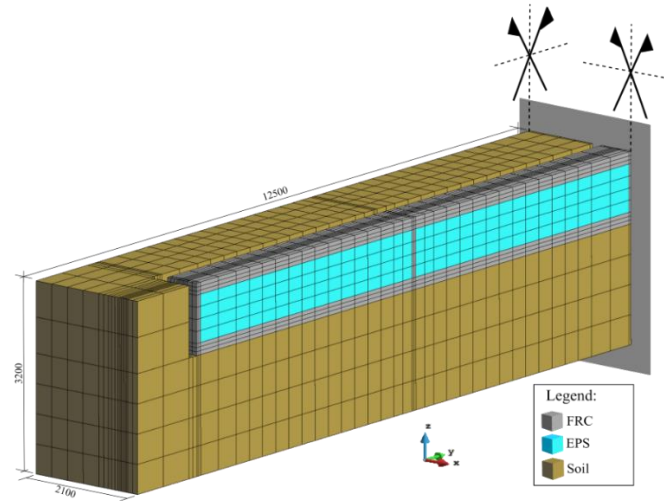
Figure 5 – Finite element mesh of ¼ of the foundation and surrounding soil (dimensions in mm).
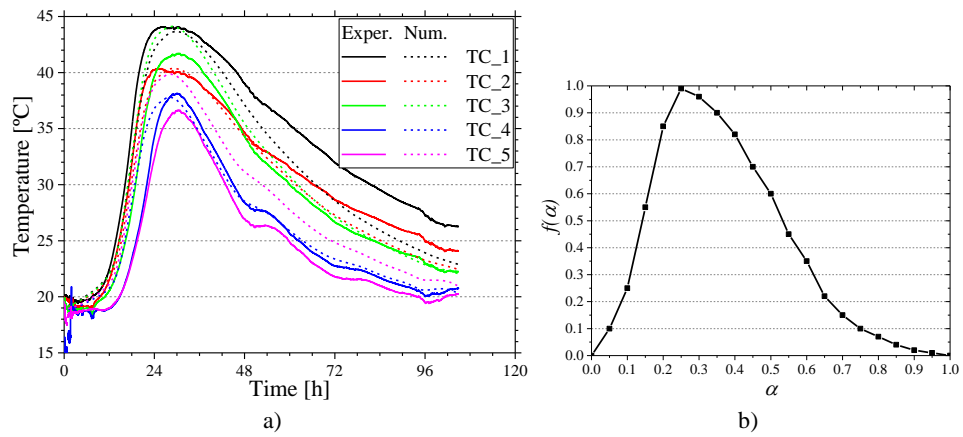

a)

b)

Figure 6 – a) Comparison between temperature registered by the thermocouples in the experimental tests and predicted numerically in their locations; b) Derived normalized heat generation rate.
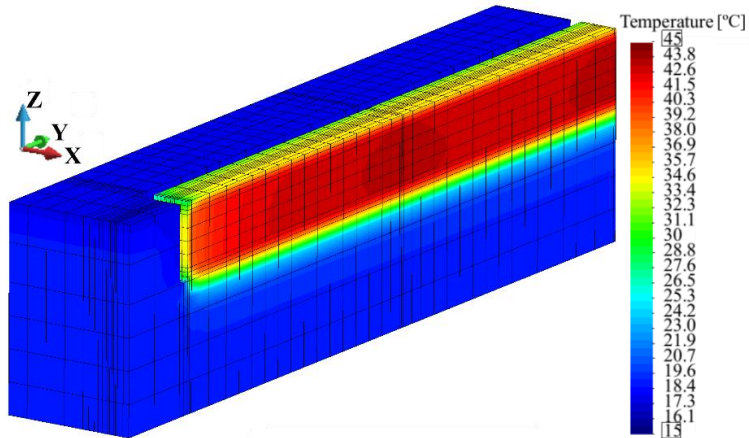
Figure 7 – Temperature field in the HRC foundation at the *t*=25h after casting.

3.2 Derivation of FRC stress-crack width relationship

To simulate the fracture mode I process of the developed FRC, including its evolution since its casting stage, the stress-crack width relationship of the FRC was derived by performing an inverse analysis procedure based on the results obtained in the 3-point bending tests performed experimentally.

The inverse analysis was performed by conducting numerical simulations of the bending tests considering different sets of parameters that define the stress-crack width relationship of the FRC. The numerical simulations were conducted with the inverse analysis software COFIT, whose description can be found elsewhere [14].

The average response of the 3-point bending tests executed at the age of 21 days after casting were used to derive the parameters of a multilinear stress vs. crack width relationship that minimizes the deviation between the experimental and numerical force vs. midspan deflection response in these experimental tests.

The best fit of the stress-crack width relationship of the FRC at the age of 21 days after casting, derived by the inverse analysis procedure, considering a multilinear stress-crack width relationship with 6 branches and a quadrilinear stress-crack width relationship are presented in Figure 8a, including the FRC fracture energy (G_f). In Figure 8b is presented the comparison between the average experimental and numerical force vs. midspan deflection of the FRC prisms submitted to 3-point bending at the age of 21 days after casting.

From the inverse analysis procedure, it was also possible to obtain the modulus of elasticity of concrete that promotes the best fit between the numerical and experimental results, namely $E = 35GPa$.
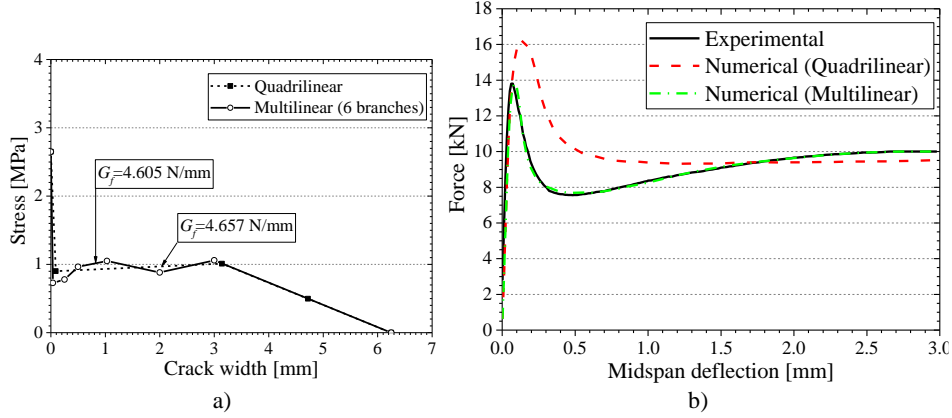
Figure 8 – a) Derived stress vs. crack width relationship of the FRC at the age of 21 days after casting; b) Comparison between the experimental and numerical force vs. midspan deflection of the FRC prisms submitted to 3-point bending at the age of 21 days after casting.

3.3 Assessment of cracking risk of the structure since early ages

To assess the cracking risk and magnitude in the early ages of the curing phase of the HRC foundation, the temperature field obtained from the thermal model is coupled with a mechanical model that can simulate the crack initiation and propagation of concrete members. A multidirectional fixed smeared crack model [15] was adopted to simulate the fracture properties of the FRC, considering the quadrilinear stress-crack width relationship derived from the inverse analysis of the 3-point bending tests of FRC prisms. To ensure that the results are independent of the finite element mesh refinement, a crack bandwidth equal to the cubic root of the integration point's volume was considered.

For simulating the crack shear stress transfer, the concept of shear retention [22] was adopted, which decreases from 1 to zero with the increase of the normal crack tensile strain according to a quadratic degradation parameter.

Considering the relatively small load level that the foundation is submitted, a linear-elastic regime was assumed for the compressive behavior of the FRC.

Surface interface finite elements were disposed between the bottom face of the foundation and the supporting soil in order to simulate their contact conditions. A total of 407 zero-thickness interface finite elements formed by 16-node quadratic elements were added to the finite element mesh presented in Figure 5 (only in the mechanical model). A Gauss-Legendre integration-scheme with 2×2 IP's was adopted for the interface elements.

The constitutive model adopted for the interface finite elements is based on the work of [16]. The model considers a linear relationship between the normal compressive stresses and vertical displacement, with a stiffness of $k_n = 50\,MPa/m$, while assuming that normal tensile stresses cannot be transferred between the faces in contact simulated by the interface finite elements. In addition, the model admits a nonlinear response

between the shear stresses and sliding of the interface ($\tau - s$). The values of the parameters defining this law were based on the information collected in [17], considering that the interface between the foundation and soil is formed by a double layer of polyethylene sheets.

In order to reduce the time to perform the transient mechanical analysis, the elements to simulate the surrounding soil of the foundation were removed and were replaced by supports in the bottom nodes of the interface finite elements.

The evolution of the mechanical properties of the concrete with time was considered in the mechanical transient analysis, by adopting a concrete maturity model coupled with the concept of equivalent age proposed in [18].

The maturity model adopts the recommendations of Eurocode 2 to simulate the evolution of the tensile strength and modulus of elasticity with time. In addition, it adopts the relationship proposed by [10] that expresses the evolution with time of the fracture energy of the concrete matrix. The maturity model evaluates the tensile strength, modulus elasticity and fracture energy at a specified time after casting as a function of the value of these properties at 28 days of age, and according to the employed type of cement.

The values of the mechanical properties at 28 days were estimated from the inverse analysis procedure of the results of the tests performed at 21 days after casting, and are presented in Table 1.

Table 1 – Estimated values of FRC mechanical properties for t=28 days.

f_{ct} [MPa]	G_f [N/mm]	E [GPa]
2.735	3.640	35.326

The model described in [18] was adopted for the simulation of the concrete aging creep behavior. Due to the inexistence of creep compliance curves for the concrete mixture under study, the B4 model is adopted to predict the creep behavior of the concrete for three loading ages $t_0 = \{1, 3, 5\}$ days, based on concrete strength performance. The creep compliance curves are then used to estimate the creep response of concrete for any loading age, considering 7 Kelvin chains with the retardation times $\tau = \{0.001; 0.01; 0.1; 1; 10; 100; 1000\}$ days and Young's modulus $E_0(t_0 = 1\,\text{day})$ =27 GPa, $E_0(t_0 = 3\,\text{days})$ =31 GPa and $E_0(t_0 = 5\,\text{days})$ =32 GPa.

In addition, the autogenous and drying shrinkage deformation of the FRC foundation were simulated based on the model proposed by EC2-1-1 that is available in FEMIX. It was considered that the drying shrinkage starts at $t_d = 1$ day.

In addition to the temperature field obtained from the nonlinear transient thermal analysis, the self-weight of the foundation materials was also considered in the mechanical analysis.

During the transient mechanical analysis, it was possible to detect the crack initiation and propagation in the concrete foundation. The maximum computed crack width (evaluated as the product of the maximum normal crack strain with the crack bandwidth) was about 12.9μm, near the middle section of the foundation, for the time instant t=23h

after casting. The maximum crack width is well below the maximum allowable value (0.3mm) indicated in EC2-1-1 for the serviceability limit state safety verifications for reinforced concrete structures, and do not constitute a threat to the durability of the HRC foundation.

The crack pattern of the foundation at t=23h after casting is presented in Figure 9, where it is noticeable that the cracking arises in the outer elements of the HRC foundation, as result of the stress gradient created due to thermal exchanges of heat from the FRC elements to the surrounding air.
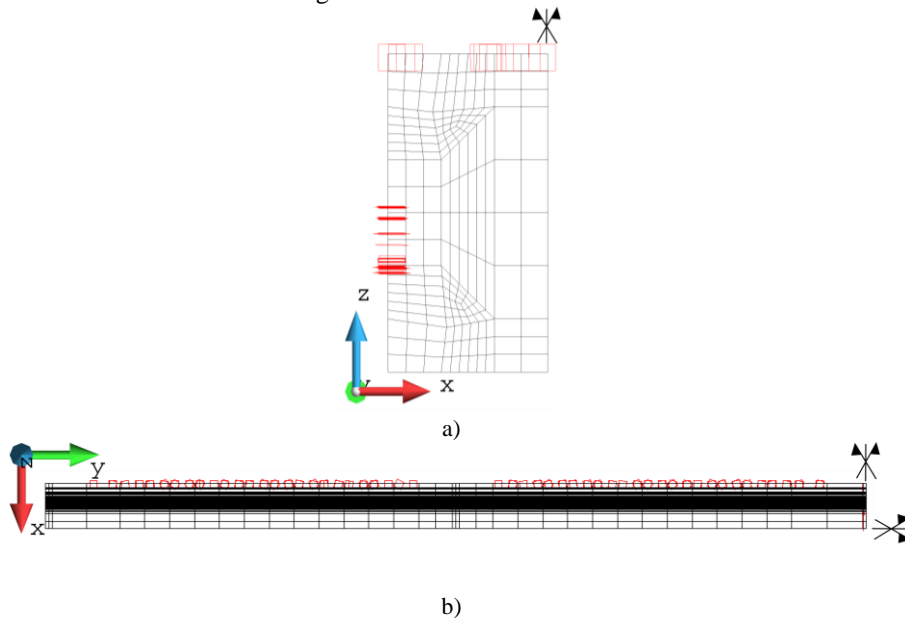

a)

b)

Figure 9 – Crack pattern at t=23 h after casting: a) XZ view of the HRC foundation (from the left extremity, y=0); b) XY (plant) view of the HRC foundation. Legend: red – opening (only cracks of width higher than 0.05mm are displayed).

In Figure 9 is presented the evolution with time of the temperature and crack width in the element of the mesh that registered the maximum crack width during the analysis. Indeed, a peak of crack width opening was observed at t=23 h, which follows the evolution with time of temperature due to cement hydration. Afterwards, with the heat dissipation and concrete volume contraction, the crack width reduces and becomes completely closed at the end of the analysis.

At the end of the mechanical transient analysis (t=105 h after casting) all the microcracks that were formed in the early stage of the concrete hardening phase end up to close, which agrees with the observation that no cracks were visible in the HRC foundation.
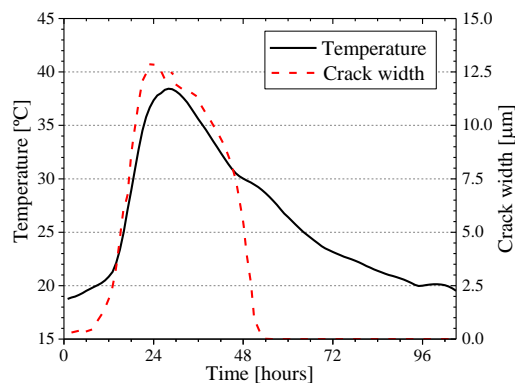
Figure 10 - Evolution of crack width time and temperature at element with maximum crack width during mechanical analysis.

4 Conclusions

In this work is presented the analysis of the cracking risk and magnitude at the early stages of the hardening phase a long jointless concrete foundation hybrid reinforced with conventional steel meshes and discrete polypropylene fibers.

A thermo-mechanical nonlinear transient analysis of the foundation was performed adopting constitutive models to simulate the cracking, viscoelasticity, shrinkage and maturity behavior of the FRC, and a model to simulate the heat development of concrete due to the cement hydration.

The strength parameters adopted in the mechanical models were derived from the results of the experimental tests. Emphasis was made on the derivation of the stress-crack width relationship of the FRC, based on an inverse analysis technique considering the results of 3-point notched beam bending tests.

In order to supply an accurate prediction of the temperature field generated by the cement hydration reactions during the early stages of concrete hardening phase, the parameters of the thermal model were calibrated based on the results collected by thermocouples installed in the concrete foundation.

The numerical simulation revealed that the hybrid reinforcement solution considered for the long jointless concrete foundation exhibited an adequate performance to limit the crack width magnitude to very small openings (less than $15\,\mu$m), while significatively reducing the conventional steel reinforcements ratio. Indeed, after the heat dissipation, these cracks have closed due to the contraction of the concrete volume. The obtained numerical results are in agreement with the visual inspection of the HRC foundation where no cracks were detected.

Acknowledgements

References

[1]   A. Domingo, C. Lázaro, and P. Serna, "CONSTRUCTION OF JCHYPAR, A STEEL FIBER REINFORCED CONCRETE THIN SHELL STRUCTURE," Varenna, Italy, Sep. 2004, p. 10.

[2]   Hai H. Dinh, "Shear behavior of steel fiber reinforced concrete beams without stirrup reinforcement," PhD Thesis, University of Michigan, Michigan, USA, 2009.

[3]   A. Conforti, F. Minelli, and G. A. Plizzari, "Wide-shallow beams with and without steel fibres: A peculiar behaviour in shear and flexure," *Compos. Part B Eng.*, vol. 51, pp. 282–290, Aug. 2013, doi: 10.1016/j.compositesb.2013.03.033.

[4]   J. A. O. Barros, "Comportamento do betão reforçado com fibras - análise experimental e simulação numérica / Behavior of fiber reinforced concrete - experimental and numerical analysis," PhD Thesis, Department of Civil Engineering, FEUP, Portugal, 1995.

[5]   J. A. O. Barros and J. Sena-Cruz, "Fracture energy of steel fiber-reinforced concrete," *Mech. Compos. Mater. Struct.*, vol. 8, no. 1, pp. 29–45, 2001.

[6]   fib-federation internationale du beton, *fib Model Code for Concrete Structures 2010*. John Wiley & Sons, 2013.

[7]   European Committee for Standardization, *Testing hardened concrete - Parte 3: Compressive strength of test specimens*, vol. EN 12390-3. 2009.

[8]   European Committee for Standardization, *Test method for metallic fibered concrete - Measuring the flexural tensile strength (limit of proportionality (LOP), residual)*, vol. EN 14651. 2005.

[9]   European Committee for Standardization, *Eurocode 2: Design of concrete structures Part 1-1: General rules and rules for buildings*, vol. NP EN 1992-1-1. 2010.

[10]   A. Ventura-Gouveia, "Constitutive models for the material nonlinear analysis of concrete structures including time dependent effects," PhD Thesis, Department of Civil Engineering, University of Minho, 2011.

[11]   H. W. Reinhardt, J. Blaauwendraad, and J. Jongedijk, "Temperature development in concrete structures taking account of state dependent properties," 1982.

[12]   M. Â. D. Azenha, "Numerical simulation of the structural behaviour of concrete since its early ages," PhD Thesis, aculdade de Engenharia. Universidade do Porto, School of Eneginering. University of Tokyo., 2012.

[13]   A. F. M. Azevedo, J. A. O. Barros, J. Sena-Cruz, and A. V. Gouveia, *Femix 4.0*. Porto: Consoft, 2013.

[14]   L. M. P. Matos, B. Barros J. A. O., A. Ventura-Gouveia, and R. A. B. Calçada, "A new inverse analysis approach for predicting the fracture mode I parameters of FRC from three

point notched beam bending tests and round panel tests," Technical Report 20-DEC/E-40, 2020.

[15] A. V. Gouveia, J. A. Barros, Á. F. Azevedo, and J. Sena-Cruz, "Multi-fixed smeared 3d crack model to simulate the behavior of fiber reinforced concrete structures," presented at the CCC 2008 - Challenges for Civil Construction, Porto, 2008, [Online]. Available: http://hdl.handle.net/1822/12802.

[16] Tiago Valente, "Advanced tools for design and analysis of fiber reinforced concrete structures," PhD Thesis, University of Minho, Guimarães, Portugal, 2019.

[17] W. S. Chia, B. F. McCullough, and N. H. Burns, "Field evaluation of subbase friction characteristics," Center of Transportation Research Bureau of Engineering Research The University of Texas at Austin, Research Report 401-5, 1986. Accessed: May 24, 2016. [Online]. Available: http://library.ctr.utexas.edu/digitized/texasarchive/phase2/401-5-CTR.pdf.

[18] Ventura-Gouveia, A, Barros, J.A.O., and Azevedo, A.F.M., "Thermo-mechanical model for the material nonlinear analysis of cement based materials," presented at the 9th international conference on fracture mechanics of concrete and concrete structures, Berkeley, California USA, 2016.